

Novel Cytotoxic Topoisomerase II Inhibiting Pyrroloiminoquinones from Fijian Sponges of the Genus *Zyzzya*

Derek C. Radisky,[†] Evette S. Radisky,[†] Louis R. Barrows,[§] Brent R. Copp,[†] Robert A. Kramer,[†] and Chris M. Ireland^{*,†,1}

Contribution from the Department of Medicinal Chemistry, College of Pharmacy, Department of Pharmacology and Toxicology, College of Pharmacy, University of Utah, Salt Lake City, Utah 84112, and American Cyanamid Company, Lederle Laboratories, Pearl River, New York 10965. Received July 21, 1992

Abstract: We present the isolation and characterization of seven novel [natural] pyrroloiminoquinones, the makaluvamines A-F (1-6), makaluvone (7), and the known compounds discorhabdin A (8) and damirone B (9) from the Fijian sponge *Zyzzya cf. marsailis*. The makaluvamines exhibit potent in vitro cytotoxicity toward the human colon tumor cell-line HCT 116, show differential toxicity toward the topoisomerase II sensitive CHO cell-line xrs-6, and inhibit topoisomerase II in vitro. This activity may be mediated by intercalation into DNA and single-stranded breakage. Makaluvamine A and C exhibited in vivo antitumor activity against the human ovarian carcinoma Ovar3 implanted in athymic mice. The makaluvamines suggest a plausible interrelationship between the batzelline/isobatzelline and discorhabdin/prianosin classes of compounds.

Marine sponges and ascidians have proven to be a valuable source of a variety of biologically active secondary metabolites;² recently, a series of publications described a new class of highly cytotoxic pyrroloiminoquinones based on a pyrrolo[4,3,2-de]-quinoline skeleton: batzellines and isobatzellines, isolated from the Caribbean sponge *Batzella* sp.,³ damirones, isolated from the Palauan sponge *Damiria* sp.,⁴ discorhabdins, isolated from New Zealand sponges of the genus *Latrunculia*,⁵ prianosins, isolated from the Okinawan sponge *Prianos melanos*,⁶ and most recently, wakayin, isolated from the Fijian ascidian *Clavelina* sp.⁷

As a part of our continuing search for potential antineoplastic agents from marine sources, we isolated makaluvamines A-F, makaluvone, and the known compounds damirone B and discorhabdin A from the Fijian sponge *Zyzzya cf. marsailis*.⁸ We report here the structure determination of the new compounds and preliminary evidence for the ability of this class of metabolites to inhibit the function of mammalian topoisomerase II⁹ and to inhibit the growth of human ovarian tumor in an athymic mouse model.

Isolation and Structure Determination of Makaluvamines A-F (1-6) and Makaluvone (7). Sponge specimens of *Z. cf. marsailis* were collected from coastal waters of the Fiji islands on two separate occasions. Solvent partition of the methanol extract resulted in concentration of the cytotoxic activity primarily in the chloroform layers. Silica gel flash chromatography of the chloroform soluble material followed by chromatography with lipophilic sephadex LH 20 yielded, for the first collection, makaluvamines A, B, D, E, and F (1, 2, 4, 5, and 6), makaluvone (7), and the known discorhabdin A^{5b} (9), while the second collection yielded makaluvamines A and C (1 and 3) and the known compound damirone B (8).

Makaluvamine A (1) showed a protonated molecular ion at m/z 202.0978 by HR FAB mass spectral analysis, in agreement with the molecular formula C₁₁H₁₂N₃O (Δ 1.2 mmu). The ¹³C NMR (DMSO-*d*₆) spectrum contained 11 resonances (Table I). A coupled ¹³C NMR experiment established the multiplicities of the carbon resonances while an ¹H-detected heteronuclear multiple quantum coherence (HMQC)¹⁰ NMR experiment permitted assignment of the attached protons (Table I). Characteristic pyrroloiminoquinone resonances in the ¹H NMR spectrum of 1 included mutually coupled methylene signals at 3.75 ppm and 2.83 ppm (observed as triplets with $J_{HH} = 7.5$ Hz), which were attached to carbons at 42.0 and 18.0 ppm, respectively, a pyrrole C-2 proton resonance at 7.30 ppm attached to a carbon resonance at 131.0

ppm, and an olefinic proton resonance at 5.61 ppm attached to a carbon resonance at 86.4 ppm (C-6). A COSY¹¹ NMR experiment allowed placement of the methyl resonance (3.88 ppm) on the nitrogen of the pyrrole by correlation with the H-2 proton, which itself exhibited long range correlation to the upfield arm (H₂-3) of the mutually coupled methylene proton spin system. The downfield arm of the mutually coupled methylenes (H₂-4) correlated to a broad exchangeable proton at 10.44, which was assigned as H-5. The olefinic proton H-6 showed COSY correlations to both of the exchangeable signals at 8.37 ppm and 9.09 ppm, which were assigned as diastereotopic protons on the primary amine N-7. Structure 1 was further supported by results of ¹H-detected heteronuclear multiple bond ¹H-¹³C correlation (HMBC)¹² experiments. The pyrrole carbon at δ 131.0 correlated to the *N*-methyl protons (δ 3.88) and the methylene protons H₂-3. The carbon resonance at 123.0 ppm correlated to the *N*-methyl protons and the pyrrole proton H-2, while the carbon resonance at 122.3 ppm correlated to the protons H-2 and H-6, allowing

(1) NIH Career Development Awardee, 1987-1992.

(2) (a) Ireland, C. M.; Copp, B. R.; Foster, M. P.; McDonald, L. A.; Radisky, D. C.; Swersey, J. C. In *Pharmaceutical and Bioactive Natural Products*; Zaborsky, O. R., Attaway, D., Eds.; Plenum Press: New York, 1986; *Marine Biotechnology*; Vol. 1, in press. (b) Ireland, C. M.; Roll, D. M.; Molinski, T. F.; McKee, T. C.; Zabriskie, T. M.; Swersey, J. C. In *Biomedical Importance of Marine Organisms*; Fautin, D. G., Ed.; California Academy of Sciences: San Francisco, 1988; No. 13, pp 41-57.

(3) (a) Sun, H. H.; Sakemi, S.; Burren, N.; McCarthy, P. *J. Org. Chem.* 1990, 55, 4964. (b) Sakemi, S.; Sun, H. H.; Jefford, C. W.; Bernardinelli, G. *Tetrahedron Lett.* 1989, 30, 2517.

(4) Stierle, D. B.; Faulkner, D. J. *J. Nat. Prod.* 1991, 54, 1131.

(5) (a) Perry, N. B.; Blunt, J. W.; McCombs, J. D.; Munro, M. H. G. *J. Org. Chem.* 1986, 51, 5476. (b) Perry, N. B.; Blunt, J. W.; Munro, M. H. G. *Tetrahedron* 1988, 44, 1727. (c) Perry, N. B.; Blunt, J. W.; Munro, M. H. G.; Higa, T.; Sakai, R. *J. Org. Chem.* 1988, 53, 4127. (d) Copp, B. R. Ph.D. Thesis, University of Canterbury, New Zealand, 1989; Chapter 5. (e) Blunt, J. W.; Munro, M. H. G.; Battershill, C. N.; Copp, B. R.; McCombs, J. D.; Perry, N. B.; Prinsep, M. R.; Thompson, A. M. *New J. Chem.* 1990, 14, 761.

(6) Kobayashi, J.; Cheng, J.; Ishibashi, M.; Nakamura, H.; Ohizumi, Y.; Hirata, Y.; Sasaki, T.; Lu, H.; Clardy, J. *Tetrahedron Lett.* 1987, 28, 4939. Cheng, J.; Ohizumi, Y.; Wälchli, M. R.; Nakamura, H.; Hirata, Y.; Sasaki, T.; Kobayashi, J. *J. Org. Chem.* 1988, 53, 4621. Kobayashi, J.; Cheng, J.; Yamamura, S.; Ishibashi, M. *Tetrahedron Lett.* 1991, 32, 1227.

(7) Copp, B. R.; Ireland, C. M.; Barrows, L. R. *J. Org. Chem.* 1991, 56, 4596.

(8) Personal communication, Van Soest.

(9) A full disclosure of the biological activities of these compounds will be presented elsewhere.

(10) Summers, M. F.; Marzilli, L. G.; Bax, A. *J. Am. Chem. Soc.* 1986, 108, 4285.

(11) Rance, M.; Sørensen, O. W.; Bodenhausen, G.; Wagner, G.; Ernst, R. R.; Würthrich, K. *Biochem. Biophys. Res. Commun.* 1983, 117, 429.

(12) Bax, M.; Summers, M. F. *J. Am. Chem. Soc.* 1986, 108, 2093. Bax, A.; Asqalos, A.; Dinya, Z.; Sudo, K. *J. Am. Chem. Soc.* 1986, 108, 8056.

[†] American Cyanamid Co.

[†] Department of Medicinal Chemistry.

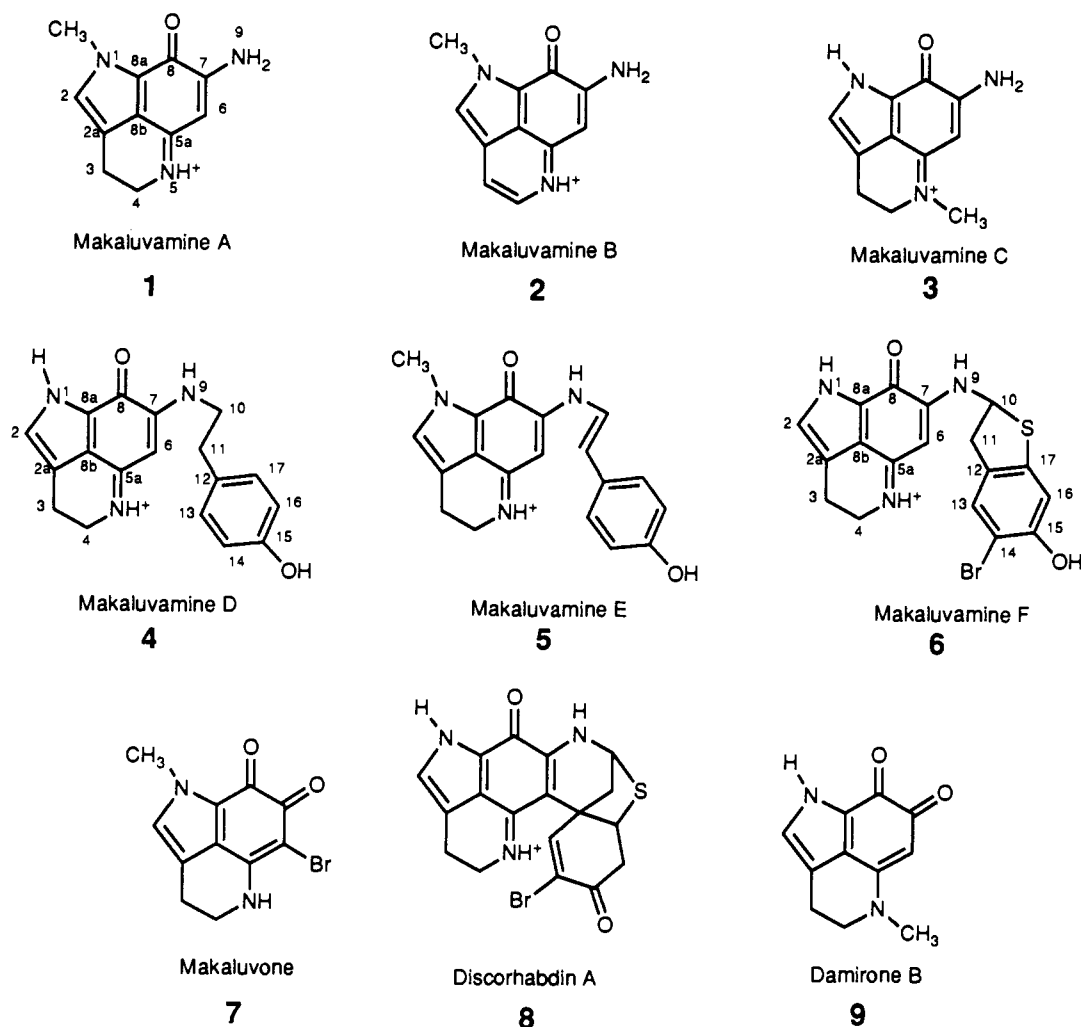
[§] Department of Pharmacology and Toxicology

Table I^c

	makaluvamine A (1)		makaluvamine B (2)		makaluvamine C (3)		makaluvamine D (4)		makaluvamine E (5) ^b		makaluvamine F (6)		makaluvone (7)		damirone B (9) ^a	
	¹ H	¹³ C	¹ H	¹³ C	¹ H	¹³ C	¹ H	¹³ C	¹ H	¹³ C	¹ H	¹³ C	¹ H	¹³ C	¹ H	¹³ C
N-Me	3.88	35.8 (q, <i>J</i> = 141)	4.26	37.0 (q, <i>J</i> = 140)	3.31	39.0 (q, <i>J</i> = 144)			3.97	37.0 (q, <i>J</i> = 142)			3.82	35.5 (a, <i>J</i> = 142)	3.03	37.4 (q, <i>J</i> = 133)
1					13.10		13.08				13.17				12.40	
2	7.30	131.0 (d, <i>J</i> = 189)	8.15	131.1 (d, <i>J</i> = 195)	7.28 (d, <i>J</i> = 1.0)	126.6 (d, <i>J</i> = 191)	7.32 (br s)	126.9 (d, <i>J</i> = 185)	7.10	132.4 (d, <i>J</i> = 190)	7.32 (br d)	126.7 (d, <i>J</i> = 191)	7.15	129.4 (d, <i>J</i> = 191)	7.06 (d, <i>J</i> = 2.5)	124.0 (d, <i>J</i> = 190)
2a		117.8		122.2		123.4		118.7		120.2		118.7		123.6		124.9
3	2.83 (t, <i>J</i> = 7.5)	18.0 (t, <i>J</i> = 132)	7.40 (d, <i>J</i> = 5.5)	111.0 (d, <i>J</i> = 168)	2.92 (t, <i>J</i> = 7.5)	18.9 (t, <i>J</i> = 131)	2.87 (t, <i>J</i> = 7.0)	17.9 (t, <i>J</i> = 127)	2.94 (t, <i>J</i> = 7.5)	20.1 (t, <i>J</i> = 135)	2.91 (t, <i>J</i> = 7.5)	17.9 (t, <i>J</i> = 134)	2.71 (t, <i>J</i> = 7.0)	18.9 (t, <i>J</i> = 131)	2.79 (t, <i>J</i> = 7.0)	19.7 (t, <i>J</i> = 134)
4	3.75 (t, <i>J</i> = 7.5)	42.0 (t, <i>J</i> = 142)	8.21 (dd, <i>J</i> = 5.5, 1.0)	141.3 (d, <i>J</i> = 177)	3.90 (t, <i>J</i> = 7.5)	52.6 (t, <i>J</i> = 146)	3.80 (t, <i>J</i> = 7.0)	41.8 (t, <i>J</i> = 139)	3.86 (t, <i>J</i> = 7.5)	44.6 (t, <i>J</i> = 143)	3.88 (t, <i>J</i> = 7.5)	42.9 (t, <i>J</i> = 141)	3.57 (t, <i>J</i> = 7.0)	42.0 (t, <i>J</i> = 142)	3.59 (t, <i>J</i> = 7.0)	51.2 (t, <i>J</i> = 145)
5	10.44		6.43				10.45				11.22		8.14			
5a		156.0		148.1		155.7		157.1		158.8		151.1		150.4		153.5
6	5.61	86.4 (d, <i>J</i> = 164)		98.5 (d, <i>J</i> = 159)	5.73	85.5 (d, <i>J</i> = 165)	5.46	84.1 (d, <i>J</i> = 162)	5.8	87.6 (d, <i>J</i> = 164)	5.54	88.0 (d, <i>J</i> = 163)		87.3	5.12	92.5 (d, <i>J</i> = 167)
7		156.7		150.2		156.5		153.1		149.2		157.6		168.7		170.4
8		168.2		167.1		167.4		167.4		169.7		167.6		171.7		178.3
8a		123.0		119.0		117.9		123.8		125.6		124.1		123.5		124.4
8b		122.3		117.9		123.2		122.6		124.3		121.6		116.7		116.4
9	8.37 9.09		6.32		8.65 9.53		8.99 (br t)				9.20 (d, <i>J</i> = 7.5)					
10							3.46 (br m)	45.1 (t, <i>J</i> = 139)	7.19 (d, <i>J</i> = 14.5)	121.8 (d, <i>J</i> = 172)	5.79 (br m)	63.6 (d, <i>J</i> = 161)				
11							2.78 (t, <i>J</i> = 7.0)	32.4 (t, <i>J</i> = 127)	6.79 (d, <i>J</i> = 14.5)	125.6 (d, <i>J</i> = 152)	3.51 (dd, <i>J</i> = 16.5, 7.5, 3.70 (dd, <i>J</i> = 16.5, 2.5)	39.2 (t, <i>J</i> = 133)				
12								128.3		128.4		130.1				
13							7.03 (d, <i>J</i> = 7.5)	129.6 (d, <i>J</i> = 162)	7.33 (d, <i>J</i> = 8.0)	129.7 (d, <i>J</i> = 157)	7.37 (s)	129.1 (d, <i>J</i> = 164)				
14							6.68 (d, <i>J</i> = 7.5)	115.2 (d, <i>J</i> = 164)	6.75 (d, <i>J</i> = 8.0)	117.3 (d, <i>J</i> = 159)		105.3				
15								156.0		159.9	6.81 (s)	153.5				
16							6.68	115.2	6.75	117.3		109.4 (d, <i>J</i> = 163)				
17							7.03	129.6	7.33	129.7		138.7				

^aUnassigned spectral data for damirone B have been previously reported. ^bNMR spectra of makaluvamine E were performed in CD₃OD; all other spectra were performed in DMSO-*d*₆. ^c*J* values are given in hertz.

Chart I



assignment of these carbons as C-8a and C-8b, respectively. The carbon resonance at 117.8 ppm correlated to the protons H-2, H₂-3, and H₂-4, allowing assignment as C-2a, while the resonance at 156.7 ppm correlated to the protons H₂-3 and H₂-4, indicating it to be the imine carbon 5a. The carbon resonance at 168.2 ppm correlated to both of the exchangeable protons assigned to the primary amine N-9 and to the protons H-6 and H-2, allowing assignment as the carbonyl carbon C-8. The assignment of makaluvamine A as 1 is consistent with published data for a semisynthetic derivative of isobatzelline A.³

Makaluvamine B (2) showed a protonated molecular ion at *m/z* 200.0827 by HR mass spectral analysis which agreed with the molecular formula C₁₁H₁₀N₃O (Δ 0.3 mmu). The ¹³C and ¹H NMR (DMSO-*d*₆) spectral data (Table I) were similar to the data observed for makaluvamine A (1), with the major exception that the pair of mutually coupled methylene signals were replaced by a pair of mutually coupled olefinic methines (*J*_{HH} = 5.5 Hz). Additionally, the two N-9 protons now had coalesced at 6.32 ppm. COSY and HMBC NMR experiment results were entirely consistent with structure 2 for makaluvamine B.

Makaluvamine C (3) showed a protonated molecular ion at *m/z* 202.0979 by HR mass spectral analysis, consistent with the molecular formula C₁₁H₁₂N₃O (Δ 0.1 mmu). COSY, HMQC, and HMBC NMR (DMSO-*d*₆) experiments indicated a pyrroloiminoquinone substructure similar to makaluvamine A. In this case, however, the pyrrole *N*-methyl of makaluvamine A was replaced by an NH proton at 13.10 ppm, while the NH-5 proton was replaced by a methyl signal, with the carbon at 39.0 ppm and protons at 3.31 ppm. A COSY NMR experiment defined the proton spin systems of the pyrroloiminoquinone fragment. The indole NH proton, observed at δ 13.10, correlated to H-2 (δ 7.28),

which in turn exhibited a long-range correlation to the upfield arm of the mutually coupled methylenes H₂-3 (δ 2.92) and H₂-4 (δ 3.90), which were observed as triplets with *J*_{HH} = 7.5 Hz. The H-6 proton (δ 5.73) exhibited long-range correlations to the H₂-9 protons at 8.65 and 9.53 ppm. An HMQC NMR experiment established all of the ¹*J*_{CH} correlations, and an HMBC NMR experiment optimized for ^χ*J*_{CH} = 10 Hz (three-bond) confirmed the assignment of the pyrroloiminoquinone substructure.

Makaluvamine D (4) showed a protonated molecular ion at *m/z* 308.1407 by HR mass spectral analysis. Consistent with the molecular formula C₁₈H₁₈N₃O₂ (Δ 0.8 mmu), the ¹³C NMR (DMSO-*d*₆) spectrum contained 18 resonances, and the ¹H NMR spectrum showed evidence for 18 protons (Table I). COSY, HMQC, and HMBC NMR experiments indicated a pyrroloiminoquinone substructure similar to makaluvamine A (1), although N-1 was substituted with a hydrogen instead of a methyl, as in makaluvamine C. A COSY NMR experiment demonstrated a continued spin system from NH-9 (δ 8.99) to a pair of mutually coupled methylene resonances H₂-10 (a multiplet at δ 3.46) and H₂-11 (a triplet at δ 2.78 with *J*_{HH} = 7.0 Hz). An HMQC NMR experiment allowed assignment of the associated methylene carbon resonances (C-10, 45.1 ppm; C-11, 32.4 ppm), while correlations observed in an HMBC NMR experiment from C-7 (δ 153.1) to H₂-10, and C-10 to NH-9 provided further evidence for the attachment of C-10 to N-9. The remaining data, comprised of methine carbon signals at 115.2 and 129.6 ppm attached to a set of proton doublets (*J*_{HH} = 7.5 Hz) integrating for two protons each, at 6.68 and 7.03 ppm, respectively, and quaternary carbon signals at 128.3 and 156.0 ppm suggested the presence of a *para*-substituted phenol.¹³ HMBC correlations were fully consistent with attachment of a *p*-hydroxy phenethyl unit to N-9, thus

completing the assignment of 4.

Makaluvamine E (5) showed a protonated molecular ion at m/z 320.1384 by HR mass spectral analysis, indicating a molecular formula of $C_{19}H_{18}N_3O_2$ (Δ 1.5 mmu). COSY, HMQC, and HMBC NMR (CD_3OD) experiments established the presence of the pyrroloiminoquinone substructure of makaluvamine A which was further substituted at N-9. The data for the remainder of the structure was similar to that observed for makaluvamine D (4), i.e., mutually coupled methine proton doublets, each integrating for two protons, at 7.33 and 6.75 ppm ($J_{HH} = 8.0$ Hz), attached to carbons at 129.7 and 117.3 ppm, respectively, and quaternary carbons at 128.4 and 159.9 ppm. In the case of makaluvamine E (5), however, the resonances of the two mutually coupled methylenes C-10 and C-11 had been replaced by a mutually coupled pair of olefinic protons at 7.19 and 6.79 ppm, bound to carbon resonances at 121.8 and 125.6 ppm, respectively. A J_{HH} of 14.0 Hz between the olefinic protons indicated an *E* olefinic geometry. HMBC NMR correlations observed between the methine proton at 7.19 ppm and C-7 (δ 149.2) and the quaternary carbon at 128.4 ppm, as well as between the methine proton at 6.79 ppm and the carbon resonance at 129.7 ppm, completed the assignment of 5 (Table I).

Makaluvamine F (6) showed a protonated molecular ion at m/z 416.0068 by HR FAB mass spectral analysis. In agreement with the molecular formula $C_{18}H_{15}^{79}BrN_3O_2S$ (Δ 0.1 mmu), 18 resonances were observed in the ^{13}C NMR ($DMSO-d_6$) spectrum of 6 (Table I). The assignment of the pyrroloiminoquinone substructure revealed that the pyrrole nitrogen was again unsubstituted, as seen in makaluvamine D. The remaining substructure, C_8H_6BrSO (five unsaturations), was composed of four quaternary carbons at 130.1, 138.7, 105.3, and 153.5 ppm, three methines, and one methylene. An HMQC NMR experiment established that a methine proton at 5.79 ppm was attached to a carbon at 63.6 ppm, a pair of diastereotopic methylene protons at 3.51 ($J_{HH} = 16.5, 7.5$ Hz) and 3.70 ppm ($J_{HH} = 16.5, 2.5$ Hz) attached to the carbon at 39.2 ppm, an olefinic proton at 7.37 ppm attached to the carbon at 129.1 ppm, and an aromatic proton at 6.81 attached to the carbon at 109.4 ppm. A $^1H-^1H$ COSY NMR experiment established the proton-proton connectivities present in this substructure. The exchangeable proton NH-9 (δ 9.20) correlated to the 5.79 ppm methine proton, which correlated to the diastereotopic methylene protons, which in turn long-range correlated to both of the aromatic proton resonances. HMBC NMR experiments optimized for $^2J_{CH} = 10$ Hz indicated that these protons were located on a 2,3,5,6-tetra-substituted phenyl ring. The proton at 6.81 ppm (H-16) gave strong correlations to carbon resonances at 130.1 and 105.3 ppm and weak correlations to carbon resonances at 138.7 and 153.5 ppm, while the proton at 7.37 ppm gave strong correlations to the carbons at 138.7 and 153.5 ppm. The chemical shifts of the carbon resonance at 153.5 ppm as well as the two ortho carbons at 105.3 and 109.4 ppm are consistent with the presence of a hydroxyl substituent. A bromine substituent, required by the molecular formula, was consistent with the substantial upfield shift observed for the 105.3 ppm carbon, while the chemical shift of the carbon resonance at 130.1 ppm was consistent with an alkyl substituent para to a hydroxyl substituent. Finally, the chemical shift of the carbon resonance at 138.7 ppm (C-17) suggested a thioether linkage. The chemical shift of the methine carbon C-10 (63.6 ppm) and its large carbon-proton coupling constant ($^1J_{CH} = 161$ Hz) suggested the presence of two heteroatom substituents. Furthermore, the proton at 5.79 ppm displayed COSY correlations to NH-9 and HMBC correlations to the carbon at 138.7 ppm. This evidence suggested the placement of the methine carbon as C-10, between N-9 and the sulfur substituent on C-17. The connectivity of the methylene carbon was established by the COSY-derived spin system and HMBC correlations between the diastereotopic protons H₂-11 and C-7, C-10, C-12, and C-14. The positioning of the methylene group as C-11 completed the structure of makaluvamine F (6).

Makaluvone (7) showed molecular ions at m/z 279.9856 and 281.9839 (Δ 0.8 mmu and Δ 0.9 mmu for $C_{11}H_9^{79}BrN_2O_2$ and $C_{11}H_9^{81}BrN_2O_2$, respectively) and (M-CO)⁺ ions at m/z 251.9934

and 253.9892 (Δ 3.5 mmu and Δ 0.7 mmu for $C_{10}H_9^{79}BrN_2O$ and $C_{10}H_9^{81}BrN_2O$, respectively). The ^{13}C and 1H NMR ($DMSO-d_6$) data (Table I) were similar to the data observed for damirone B,⁴ with the important exceptions that N-5 was now unsubstituted, N-1 was substituted with a methyl, and H-6 was absent from the proton spectrum. COSY experiments established the proton backbone of the left side of the molecule: the pyrrole *N*-methyl protons (3.82 ppm) exhibited a long-range correlation to H-2 (7.15 ppm), which in turn correlated to H₂-3 (2.71 ppm), while H₂-4 (3.57 ppm) correlated to NH-5 (8.14 ppm). An HMQC experiment permitted assignment of the protonated carbons, while HMBC experiments allowed assignment of all but two carbons. The carbon resonance at 123.5 ppm correlated to both the pyrrole *N*-methyl protons and H-2, while the carbon resonance at 116.7 ppm correlated to H-2, H₂-3, and H₂-4, allowing assignment as C-8a and C-8b, respectively. The carbon resonance at 123.6 correlated to H-2 and H₂-3, allowing assignment as C-2a, while the carbon resonance at 150.4 correlated to H₂-4, indicating it as C-5a. A correlation observed between the carbon resonance at 171.7 ppm and H-2 permitted its assignment as C-8. The remaining carbons (168.7 and 87.3 ppm) were assigned by comparison with batzelline C.^{3b} Replacement of the chlorine at C-6 in batzelline C with a bromine in makaluvone is consistent with the upfield shift observed for C-6 (87.3 ppm for makaluvone, 96.9 ppm for batzelline C), while the chemical shifts for C-7 are very similar for both molecules (168.7 ppm for makaluvone, 169.1 ppm for batzelline C). The chemical shifts of all carbons other than C-6 were likewise similar between batzelline C and makaluvone.

Bioactivity

Cytotoxicity testing against the human colon tumor cell line HCT-116 (Table II) determined that discorhabdin A is the most cytotoxic, followed closely by makaluvamine F; makaluvamine A is an order of magnitude less potent, and makaluvamines D and C exhibited a further order of magnitude reduction of cytotoxicity. Makaluvamine B, makaluvone, and damirone B were not active against HCT-116. Interestingly, makaluvamines D, E, and F and discorhabdin A demonstrate dramatically increasing cytotoxicity concurrent with increasing structural elaboration.

The cytotoxicities against xrs-6, a Chinese hamster ovary (CHO) cell line sensitive to agents that cause double-stranded breaks,¹⁴ parallel the data obtained with HCT-116 (Table II); discorhabdin A and makaluvamine F are the most potent, while makaluvamine B, makaluvone, and damirone B are much less active. However, the metabolite cytotoxicity trends are substantially different than the hypersensitivity factors (HF) obtained by comparison of the cytotoxicity against xrs-6 versus BR1 (a DNA-repair proficient CHO line).¹⁵ Specifically, makaluvamine A displays the greatest hypersensitivity factor of 9, followed by makaluvamines F, E, C, and D. These results are indicative of a mechanism of action involving DNA double-stranded breakage, an activity characteristic of topoisomerase II inhibitors.¹⁶ The known inhibitor mAMSA^{17,18} displayed a HF of 6. Interestingly, insignificant hypersensitivity factors are found for makaluvamine B, makaluvone, damirone B, and discorhabdin A.

We confirmed that the makaluvamines are topoisomerase II inhibitors using a decatenation inhibition assay. This assay measures the ability of a compound to inhibit topoisomerase II-mediated DNA strand passage; mAMSA produced 90% inhibition of DNA decatenation at 20 μ M. The makaluvamines produced decatenation inhibition values well correlated with the

(13) Experimentally derived NMR data for tyramine (Aldrich), 60 mg in $DMSO-d_6$: 1H δ 6.95 (d, 2 H, 8.5 Hz), δ 6.66 (d, 2 H, 8.5 Hz), δ 2.69 (t, 2 H, 7.5 Hz), δ 2.52 (t, 2 H, 7.5 Hz); ^{13}C δ 155.6 (s), δ 129.6 (d, 162 Hz), δ 115.1 (d, 162 Hz), δ 43.8 (t, 135 Hz), δ 38.8 (t, 125 Hz).

(14) Kemp, L. M.; Sedgwick, S. G.; Jeggo, P. A. *Mutat. Res.* **1984**, *132*, 189.

(15) Barrows, L. R.; Borchers, A. H.; Paxton, M. B. *Carcinogenesis* **1987**, *8*, 1853.

(16) Lu, L. F. *Annu. Rev. Biochem.* **1989**, *58*, 351.

(17) Abbreviations: *m*-AMSA, 4'-(9-acridinylamino)methanesulfon-*m*-aniside; PVA, poly(vinyl alcohol).

(18) (a) Baguley, B.; Denny, W.; Atwell, G.; Cain, B. J. *Med. Chem.* **1981**, *24*, 520. (b) Waring, M. *Eur. J. Cancer* **1976**, *12*, 995.

Table II. Biological Activities of Compounds from *Zyzzya cf. Marsailis*

compound	HCT 116, ^a μM	xrs-6, ^a μM (HF) ^b	decat inhibit, ^c μM	DNA K _s , mM	reductive cleavage, ^d μM	reductive potential, ^e mV
makaluvamine A	1.3	0.41 (9)	41	0.022	2.1	-200
makaluvamine B	>50	13.49 (1)	>500	0.070	181	none
makaluvamine C	36.2	5.4 (4)	420	0.013	1.2	-180
makaluvamine D	17.1	14.0 (3)	320	0.024	52	-285
makaluvamine E	1.2	1.7 (4)	310	0.0046	15	-250
makaluvamine F	0.17	0.08 (6)	25	0.021	1.1	-185
makaluvone	>50	>50 (1)	>500	1.16	>1000	-250
damirone B	>50	>50 (1)	>500	1.07	>1000	-225
discorhabdin A	0.08	0.02 (2)	>500	0.085	33	-130

^aIC₅₀. ^bHF = (IC₅₀ BR1/IC₅₀ xrs-6). ^cIC₉₀. ^d50% cleavage, (10 mM Tris-HCl, 1 mM EDTA, pH 8.0). ^eCorrected for standard hydrogen electrode, performed at constant pH 7.5.

results obtained from the xrs-6/BR1 assay. Again, makaluvamines A and F were the most potent, with inhibitory concentrations essentially the same as those observed with mAMSA. Makaluvamines C and E were an order of magnitude less active, and makaluvamines B and D, makaluvone, damirone B, and discorhabdin A were all inactive. These values indicate that topoisomerase inhibition is associated with the iminoquinone structure, as the oxidized makaluvamine B and the orthoquinones makaluvone and damirone B are all inactive. The inability of discorhabdin A to inhibit topoisomerase II is indicative that this potent cytotoxin most probably acts by a different mechanism than the makaluvamines.

Further evidence that the makaluvamines are topoisomerase II inhibitors is provided by the neutral filter elution assay, a whole cell assay for the measurement of protein-associated DNA double strand breaks consistent with the production of cleavable complexes.^{19,20} Clinically useful inhibitors of topoisomerase II act by stabilizing the DNA-topo II complex after the enzyme has induced a double strand break, temporarily preventing the enzyme from religating and releasing the DNA. This stabilized intermediate is the cleavable complex; it prevents DNA replication and induces cytotoxicity in rapidly dividing cells.²¹ A dosage of makaluvamine A equitoxic to 5 mM m-AMSA produced comparable strand scission factors (the SSF for makaluvamine A was 1.38, while the SSF for m-AMSA was 1.40).²²

Makaluvamine inhibition of topoisomerase II suggested a DNA-interactive mechanism, and the fused-ring, planar aromatic, cationically charged molecular structure is consistent with compounds known to intercalate into DNA.²³ Absorption titrations were performed by monitoring the changes in the absorbance spectra of makaluvamines A and C with increasing amounts of calf thymus DNA. Makaluvamines A and C displayed 53% and 66% absorption hypochromism, respectively, and red shifts of 6 nm; these results are comparable with known DNA intercalators.²⁴ The makaluvamines also displace intercalated ethidium bromide.²⁵ Quantitative analyses of ligand interactions at equilibrium suggest a linked function involving competitive displacement of ethidium bromide.²⁶ The experimentally determined makaluvamine-DNA

Table III. Reductive Potential and DNA Cleavage vs pH for Makaluvamines A and C

pH	MkA red Clv (μM)	MkA reduction potential ^a (mV)	MkC red Clv (μM)	MkC reduction potential ^a (mV)
5.5	>1000	-115	25	-120
6.5	530	-175	11	-155
7.5	23	-200	6.1	-180
8.5	2.2	-220	2.0	-195

^aCorrected for standard hydrogen electrode, performed at constant pH.

equilibrium constants are presented in Table II. Unsurprisingly, the uncharged orthoquinone compounds makaluvone and damirone B displayed low affinities for DNA, and all compounds with significant topo II activity had *K* values less than 30 μM.

The iminoquinone structure of the makaluvamines also suggests a mechanism involving *in vivo* activation to produce a reactive semiquinone intermediate, which in turn leads to the production of DNA single-stranded breaks; this activity is preceded by iminoquinones of the mitocene class.²⁷ Furthermore, the makaluvamines possess additional structural motifs favorable to this proposed mechanism, as both an amino group and a carbonyl functionality vinylogously substitute all the semiquinone resonance forms. Although either are excellent radical stabilizers, both constitute a captodative²⁸ or merostabilized²⁹ radical; these "push-pull"³⁰ radicals have unusual stability in some situations.³¹

The DNA cleavage activity is determined with supercoiled pBR322 DNA using a modification of previously established procedures.³² The reaction is carried out under rigorous anaerobic conditions with degassed DNA/compound mixtures to which are added degassed dithionite stock. Twenty-four hours of anaerobic incubation is followed by introduction of air and aerobic incubation for an additional 24 h. Incubated, degassed control reactions are as follows: (1) DNA only, (2) DNA and dithionite only, and (3) DNA and compound only. Only when makaluvamines were combined with dithionite was any significant DNA single-stranded scission noted; no double-stranded cleavage was observed in the reductive cleavage assay. The four active reaction mixtures that produced nicked DNA contained dithionite and compound concentrations of 100 μM, 10 μM, 1 μM, and 100 nM. Following both anaerobic and aerobic incubations, agarose gel electrophoresis is used to resolve the makaluvamine-mediated nicked DNA from the supercoiled starting material. Electronic digitization of a gel photograph, followed by graphical densitometry, quantifies the

(19) Kohn, K. W.; Ewig, R. A. G.; Erickson, L. C.; Zwelling, L. A. In *DNA Repair: A Laboratory Manual of Research Procedures*; Friedberg, E. C., Hanwalt, P. O. C., Eds.; Marcel Dekker, Inc.: New York, 1981; Vol. 1, Part B, pp 379-401.

(20) (a) Kohn, K. W.; Erickson, L. C.; Ewig, R. A. G.; Friedman, C. A. *Biochemistry* 1976, 14, 4629. (b) Spiro, I. J.; Barrows, L. R.; Kennedy, K. A.; Ling, C. C. *Radiat. Res.* 1986, 108, 146.

(21) Rowe, T. C.; Chen, G. L.; Hsiang, Y.; Liu, L. F. *Cancer Res.* 1986, 46, 2021.

(22) Although the neutral filter elution assay was not performed in the absence of proteinase K, additional data support the formation of cleavable complexes. Specifically, the makaluvamines do not cause SSBs or DSBs directly in the presence of oxygen. The Makaluvamines show enhanced toxicity toward the xrs-6 cell line but not a DNA single strand repair deficient line (EM9) or a bulky adduct sensitive line (UV20). The makaluvamines also show cross resistance to mitoxantrone induced resistant cells that express atypical MDR.

(23) Wilson, W. D.; Jones, R. L. *Adv. Pharmacol. Chemother.* 1981, 18, 177.

(24) For example: Sitali, A.; Long, E. C.; Pyle, A. M.; Barton, J. K. *J. Am. Chem. Soc.* 1992, 114, 2303.

(25) Burres, N. S.; Barber, D. A.; Gunasekera, S. P.; Shen, L. L.; Clement, J. J. *Biochemical Pharmacology* 1991, 42, 745.

(26) McGhee, J. D.; von Hippel, P. H. *J. Mol. Biol.* 1974, 86, 469.

(27) Orlemans, E. O. M.; Verboom, W.; Scheltinga, M. W.; Reinhoudt, D. N.; Lelieveld, P.; Fiebig, H. H.; Winterhalter, B. R.; Double, J. A.; Bibby, M. C. *J. Med. Chem.* 1989, 32, 1612.

(28) (a) Viehe, H. G.; Janousek, Z.; Merényi, R.; Stella, L.; Janousek, Z. *Angew. Chem., Int. Ed. Engl.* 1979, 18, 917. (b) Viehe, H. G.; Janousek, Z.; Merényi, R.; Stella, L. *Acc. Chem. Res.* 1985, 12, 148.

(29) Baldock, R. W.; Hudson, P.; Katriszky, A. R. *J. Chem. Soc., Perkin Trans. 1* 1974, 1472.

(30) Balaban, A. T.; Caproiu, M. T.; Negoita, N.; Baican, R. *Tetrahedron* 1977, 33, 2249.

(31) Benson, O.; Demirdji, S. H.; Haltiwanger, C.; Koch, T. H. *J. Am. Chem. Soc.* 1991, 113, 8879.

(32) Islam, I.; Skibo, E. B.; Dorr, R. T.; Alberts, D. S. *J. Med. Chem.* 1991, 34, 2954.

Table IV. In Vivo Antitumor Activity of Representative Pyrroloiminoquinones

compound	dose (mg/kg)	Ovcar 3 min T/C, %	P388 ILS, %
vincristine	0.8	27	>91 ^a
makaluvamine A	0.5	62	0
makaluvamine C	5.0	48 ^a	18

^aSignificant at $P > 0.05$, Student's T-Test.

amount of nicked DNA. The concentration at which reduced compounds caused single-stranded breaks in 50% of the plasmid DNA is presented in Table II. Although the inactive orthoquinone compounds makaluvone and damirone B do not produce significant reductive cleavage, it is interesting that the topoisomerase II inactive makaluvamine B, which does display DNA intercalation, does not perform substantial reductive cleavage. Furthermore, the reductive cleavage values are related to the topoisomerase II inhibition of the active compounds, as activity increases in both assays for makaluvamines D, E, and F, and makaluvamine F displays the lowest DNA-nicking concentrations.

Electrochemical studies were performed to determine that redox chemistry mediates the reductive cleavage activity. The properties of the natural products at constant pH 7.5 are presented in Table II, and the pH-dependence for makaluvamines A and C are presented in Table III. With the exception of makaluvamine B, all compounds had negative reduction potentials within biologically relevant ranges. These results demonstrate that makaluvamine-mediated reductive cleavage (and probably, topoisomerase II inhibition) depends both on ability to intercalate into DNA and produce a semiquinone radical, as nonintercalators capable of reduction, such as makaluvone and damirone B, are inactive, and makaluvamine B, an intercalator incapable of reduction, also is inactive. The pH-varied experiments with makaluvamines A and C demonstrate that both reductive cleavage and reduction potential are pH dependent and additionally display the possibility of multiple ionization states, an avenue that will be explored in a future report.

Makaluvamines A and C were subjected to two different in vivo testing protocols (Table IV): Against P388 murine leukemia, makaluvamines A and C showed only marginal life extension (expressed as percent increase in life span or percent ILS), while against the human ovarian tumor Ovcar 3 implanted in athymic mice, the makaluvamines showed substantial reduction in tumor mass (expressed as % tested tumor size/control tumor size, or T/C %). It is interesting that the makaluvamines were more effective against the solid human tumor than against the murine leukemia.

The chemistry of *Z. cf. marsailis* presented here represents the first example of the co-occurrence of unfunctionalized pyrroloiminoquinones with the highly elaborated discorhabdin A. The sequence makaluvamines D–F suggests a logical biosynthetic grid that interrelates the pyrroloiminoquinone family of compounds.

Experimental Section

General Procedures. The ¹H and ¹³C NMR spectra were obtained at 500 and 125 MHz, respectively, on a Varian Unity 500 spectrometer or an IBM AF 200 spectrometer at 200 and 50 MHz, respectively. ¹H chemical shifts are reported in ppm relative to residual undeuterated solvent. IR spectra were recorded on a Perkin-Elmer 1600 FT spectrophotometer. UV spectra were obtained in methanol on a Beckman DU-8 spectrophotometer. Optical rotations were measured with a Jasco DI-P-370 polarimeter in a 50-mL cell. High- and low-resolution FAB MS were run on a Finnigan MAT-95 high-resolution gas chromatograph-mass spectrometer with Finnigan MAT ICIS II operating system. Cyclic voltammetry was performed using a Princeton Applied Research potentiostat/galvanostat Model 273.

Extraction and Isolation Procedures. Specimens of *Z. cf. marsailis* were collected at Makalua Island in November 1986 and at Mbengga harbor in November 1990, both in the Fiji island group. The methanol extract of 72.5 g of freeze dried sample of the initial collection of sponge material was concentrated in vacuo to a volume of 500 mL and subjected to a solvent partitioning scheme.³³ Briefly, a 10% aqueous methanol solution was partitioned with hexane (3 × 500 mL). The aqueous content of the lower phase was then increased to 20% and partitioned with carbon tetrachloride (3 × 500 mL). The aqueous content of the lower phase was

further increased to 40% and partitioned with chloroform (3 × 500 mL), which was concentrated in vacuo to yield 1.02 g (1.41%) of a crude solid. Vacuum flash chromatography (60 mL sintered glass funnel, 20 g silica gel G, step gradient elution from 0 to 10% methanol/chloroform) carried out on a 468 mg portion of the chloroform-soluble residue yielded a fraction (150 mg, eluting with 7.5% methanol/chloroform/0.1% TFA) which showed ¹H NMR resonances characteristic of pyrroloiminoquinones. Further silica gel chromatography using methanol/chloroform mixtures followed by repeated chromatography with LH-20 lipophilic sephadex gel (0.1% TFA/methanol or 50% methanol/chloroform/0.1% TFA) yielded 80 mg of makaluvamine A, 18 mg of makaluvamine B, 4 mg of makaluvamine D, 6 mg of makaluvamine E, 10 mg of makaluvamine F, 6 mg of makaluvone, and 12 mg of discorhabdin A.

The methanol extract of 315 g of freeze dried sample of the second collection of *Z. cf. marsailis* sponge was extracted and solvent-partitioned similarly, yielding 45.8 mg of makaluvamine A, 187.9 mg of makaluvamine C, and 20.0 mg of damirone B.

Makaluvamine A: green solid; 80 mg (0.24% dry weight); IR (TFA salt) ν_{\max} 3231, 3042, 2930, 1674, 1606, 1203, 1130, 840, 719 cm^{-1} ; UV (MeOH) λ_{\max} 242.2 (ϵ 24 000), 348.4 nm (15 500); (MeOH + OH⁻, irreversible over time) 219.7 (ϵ 17 400), 330.1 nm (16 100); HR FAB MS m/z = 202.0978 (M + H)⁺, C₁₁H₁₂N₃O requires 202.0980; ¹H and ¹³C see Table I.

Makaluvamine B: red solid; 18 mg (0.05% dry weight); IR (TFA salt) ν_{\max} 3319, 1650, 1573, 1494, 1409, 1326, 1195, 1050, 962, 947, 826, 793 cm^{-1} ; UV (MeOH) λ_{\max} 228.0 (ϵ 9600), 441.7 nm (4800); (MeOH + OH⁻) 203.9 (ϵ 17 200), 419.2 nm (4800); HR FAB MS m/z = 200.0827 (M + H)⁺, C₁₁H₁₂N₃O requires 200.0824; ¹H and ¹³C see Table I.

Makaluvamine C: green solid; 187.9 mg (0.7% dry weight); IR (TFA salt) ν_{\max} 3850, 3741, 3063, 1741, 1671, 1646, 1606, 1516, 1415, 1338, 1296, 1193, 1132, 1036, 961, 916, 793, 721 cm^{-1} ; UV (MeOH) λ_{\max} 241.4 (ϵ 25 300), 357.5 nm (19 100); (MeOH + OH⁻) 246.3 (ϵ 20 400), 355.1 nm (16 900); HR FAB MS m/z = 202.0979 (M + H)⁺, C₁₁H₁₂N₃O requires 202.0980; ¹H and ¹³C see Table I.

Makaluvamine D: brown solid; 4 mg (0.02% dry weight); IR (TFA salt) ν_{\max} 3342, 2927, 2854, 1643, 1680, 1632, 1555, 1515, 1402, 1203, 1136, 1038, 1027, 835, 801, 757, 722 cm^{-1} ; UV (MeOH) λ_{\max} 244.7 (ϵ 22 000), 347.5 nm (10 600); (MeOH + OH⁻, irreversible over time) 243.0 (ϵ 16 800), 339.2 nm (12 100); HR FAB MS m/z = 308.14075 (M + H)⁺, C₁₈H₁₈N₃O₂ requires 308.13990; ¹H and ¹³C see Table I.

Makaluvamine E: green solid; 6 mg (0.02% dry weight); IR (TFA salt) ν_{\max} 3730, 1681, 1650, 1540, 1511, 1454, 1207, 1130, 926, 843, 800, 722, 670 cm^{-1} ; UV (MeOH) λ_{\max} 226.4 (ϵ 6200), 278.0 (8700), 333.4 (6800), 448.3 (4900), 625.9 nm (5700); (MeOH + OH⁻, irreversible over time) 313.9 (ϵ 8600), 606.7 nm (5000); HR CI MS m/z = 320.1384 (M + H)⁺, C₁₉H₁₈N₃O₂ requires 320.1399; ¹H and ¹³C see Table I.

Makaluvamine F: orange solid; 10 mg (0.03% dry weight); IR (TFA salt) ν_{\max} 3600–2800, 1681, 1633, 1537, 1485, 1433, 1396, 1337, 1318, 1256, 1203, 1134, 1026, 833, 803, 752, 720, 668 cm^{-1} ; [α]_D = -475.80° (c 0.0248, CH₂OH); UV (MeOH) λ_{\max} 246.3 (ϵ 30 200), 310.5 (10 800), 344.2 nm (14 100); (MeOH + OH⁻, irreversible over time) 324.2 nm (ϵ 17 700); HR FAB MS m/z = 416.0068 (M + H)⁺, C₁₈H₁₅⁷⁹BrN₃O₂S requires 416.0069; ¹H and ¹³C see Table I.

Makaluvone: grey solid; 10 mg (0.02% dry weight); IR (TFA salt) ν_{\max} 3728, 3263, 1681, 1597, 1555, 1535, 1451, 1394, 1207, 1333, 1054, 1028, 841, 801, 765, 722, 670 cm^{-1} ; UV (MeOH) λ_{\max} 246.3 (ϵ 10 100), 330.1 nm (5500); (MeOH + OH⁻) 246.4 (ϵ 9800), 330.1 nm (6300); HR EI MS m/z = 279.9856 (M⁺) (C₁₁H₉⁷⁹BrN₂O₂ requires 279.9848), 281.9839 (C₁₁H₉⁸¹BrN₂O₂ requires 281.9848), 251.9934 (C₁₀H₉⁷⁹BrN₂O requires 251.9899), 253.9892 (C₁₀H₉⁸¹BrN₂O requires 253.9899); ¹H and ¹³C see Table I.

Damirone B: red solid; 20 mg (0.2% dry weight); IR (TFA salt) ν_{\max} 3421, 3118, 2923, 1667, 1584, 1538, 1419, 1323, 1248, 1199, 1116, 1051, 955, 922, 821, 798, 760, 723 cm^{-1} ; UV (MeOH) λ_{\max} 242.1 (ϵ 29 500), 346.7 nm (19 500); (MeOH + OH⁻) 242.2 (ϵ 29 000), 347.5 nm (19 300); HR FAB MS m/z = 203.0820 (M + H)⁺ (C₁₁H₁₁N₂O₂ requires 203.0821); ¹H and ¹³C see Table I.

Discorhabdin A: green solid; 12 mg (0.04% dry weight); NMR, UV, IR, and [α]_D data as previously reported.

Cell Culture. The CHO cell lines were grown as monolayers in α -MEM (Gibco Laboratories) containing 10% fetal bovine serum (Biologicals), 100 units/mL of penicillin, 100 $\mu\text{g}/\text{mL}$ of streptomycin, and 240 units/mL of nystatin (Sigma). The DNA repair proficient line BR1 was developed by the selection of transfected CHO cells for growth in BDNu. These cells express the hamster gene for O⁶-alkylguanine-DNA-alkyltransferase.³⁴ The line xrs-6 was a generous gift from Dr. P. Jeggo. The cells were maintained in a humidified 5% CO₂ atmosphere at 37°.

Cytotoxicity Assays. A modification of the MTT-microtiter plate tetrazolium cytotoxicity assay³⁵ was used to evaluate xrs-6/BR1 hypersensitivity, according to previously published procedures.³⁶

Decatenation Inhibition Assay. The standard in vitro assay for topo II inhibition involves administration of the inhibitor to a buffer solution containing the topoisomerase II enzyme, ATP, and kinetoplast DNA (a highly catenated tangle of 2.5 kb DNA circles). Without inhibitory compounds, the normal activity of topo II involves binding to one DNA circle, inducing a double strand break, which the enzyme then passes through the other circle. The enzyme then religates and releases the DNA, forming two decatenated circles. Known topo II inhibitors all act by permanently stabilizing the DNA–topo II complex after the enzyme has induced a double strand break and prevent the enzyme from religating and releasing the DNA. This stabilized intermediate is the cleavable complex; it prevents DNA replication and induces cytotoxicity in rapidly dividing cells. The candidate inhibitor is administered to a series of reaction mixtures in increasing concentrations, and agarose gel electrophoresis is used to detect and quantify the activity of the topo II inhibitors. However, this assay suffers from low sensitivity, as a large number of strand-passing events is required to free a single monomer circle. For this reason, a high concentration of enzyme is required and correspondingly high concentrations of inhibitory compounds.

Topoisomerase II decatenation inhibition was performed according to a modification of previously established procedures.³⁷ Briefly, each reaction was carried out in a 0.5 mL microcentrifuge tube containing 19.5 μ L of H₂O, 2.6 μ L of 10X buffer (1X buffer contains 50 mM Tris-HCl, pH 8.0, 120 mM KCl, 10 mM MgCl₂, 0.5 mM ATP, 0.5 mM dithiothreitol, and 30 μ g BSA/mL), 1 μ L of kinetoplast DNA (0.2 μ g) (TopoGen, Columbus, OH), and 1 μ L of drug solubilized in DMSO. After mixing at 0 °C, one unit of purified avian topoisomerase II (TopoGen) was added immediately before incubation in a water bath at 34 °C for 45 min. The reactions were stopped by the addition of 5 μ L of stop buffer (5% Sarkosyl, 0.0025% bromophenol blue, 25% glycerol) and were placed on ice. DNA electrophoresis was carried out on a 1% agarose gel in TAE buffer containing ethidium bromide (0.5 μ g/mL). DNA was visualized with a Spectroline Transilluminator (Spectronics Corp., Westbury, NY) at a wavelength of 310 nm, and the gels were photographed using a Polaroid Land camera.

Neutral Filter Elution Assay. Neutral filter elution performed according to modifications of previously published procedures³⁸ detected the presence of whole cell-produced protein-associated DNA double-stranded breaks. Briefly, BR1 cells were labeled overnight with [¹⁴C]-thymidine (0.07 μ Ci/mL). After a 30-min chase in fresh complete α -MEM media, varying amounts of makaluvamine A or *m*-AMSA were added to the cultures, followed by an 18-h incubation. Control cells were treated with 3% DMSO, equal to the highest drug dose cultures. No double-stranded breaks were observed in makaluvamine A-treated cells after the standard 2-h treatment, suggesting slower uptake kinetics. Timed cytotoxicity studies determined 12–18 h for optimum makaluvamine A dose durations. After iced trypsinization, the supernatant was removed by 0 °C PBS centrifugation. The cells were counted, and 1 mL of treated cells was loaded onto 0.2 μ m polycarbonate filters. Cells were lysed with a solution containing 0.05 M glycine, 0.025 M Na₂EDTA, 2% SDS, and 0.05 Tris (pH 7.2) and subjected to proteinase-K digestion. A flow rate of 0.025 mL/min yielded 16 1.5-mL fractions. Radioactivity

remaining on the filters and in each fraction was determined using a liquid scintillation counter, and strand scission factors were calculated by previously published procedures.²⁰

Reaction of Makaluvamines with Plasmid DNA. Following both incubations, the presence of nicking was determined by agarose gel electrophoresis, carried out in 0.04 M Tris/acetate pH 8.0 buffer containing 1 mM EDTA. Agarose gel (SeaKem ME, FMC BioProducts) was prepared in the same buffer at 1.0%. After electrophoresis, the gel was soaked in 0.5 μ g/mL ethidium bromide and visualized by transillumination. A photograph was electronically digitized (Abatton) and quantified by graphical densitometry (NIH Image).

Cyclic Voltammetry. Electrochemistry was performed on a gold button working electrode with a silver/silver chloride reference electrode and a platinum wire auxiliary electrode. All measurements were performed at ambient temperature on thoroughly degassed samples, and are corrected for standard hydrogen electrode. Buffer solutions were prepared as follows: pH 5.5 (NaH₂PO₄·H₂O 6.22 mg/mL, Na₂HPO₄ (anhydrous) 0.232 mg/mL, Na₂EDTA 0.375 mg/mL), pH 6.5 (NaH₂PO₄·H₂O 3.28 mg/mL, Na₂HPO₄ (anhydrous) 1.24 mg/mL, Na₂EDTA 0.375 mg/mL), pH 7.5 (NaH₂PO₄·H₂O 0.575 mg/mL, Na₂HPO₄ (anhydrous) 2.17 mg/mL, Na₂EDTA 0.375 mg/mL), pH 8.5 (NaH₂PO₄·H₂O 0.061 mg/mL, Na₂HPO₄ (anhydrous) 23.5 mg/mL, Na₂EDTA 0.375 mg/mL).

In Vivo Antitumor Activity. Makaluvamines A and C were tested for in vivo antitumor activity against two sensitive tumor models: (1) the Ovar3 human ovarian carcinoma grown as a subcutaneous solid tumor in Balb/C nu/nu athymic (i.e., nude) mice and (2) the P388 murine leukemia grown as an ascites tumor in conventional immune competent mice. Antitumor activity in the solid tumor model was assessed by comparing the size of the treated tumors (T) to that of the control tumors (C) over a 4-week period and calculating the minimum T/C \times 100% (i.e., the smallest size the tumor obtained in the treated animals relative to the control, the smaller the number the more active the compound). Activity in the murine ascites tumor model is calculated as percent increase in Median Life Span (%ILS) compared to control animals. All compounds were initially tested at three different dose levels on a day 1, 5, 9 schedule (day one after P388 ip inoculation; day one after staging for the Ovar3 solid tumor). Compounds were administered by ip treatment at the optimum dose. Vincristine was used as a positive control.

Acknowledgment. B.R.C. thanks the New Zealand-United States Education Foundation for a Fulbright Travel Award. We thank the Ministry of Home Affairs, Fiji, and the crew of the Mollie Dean for assistance in the collection. We thank Dr. Martin Rodi for expert assistance with cyclic voltammetry and Dr. Walter Ellis for many discussions. Also, we thank Dr. Elliot Rachlin for excellent mass spectrometry service. NIH Grant CA 36622 supported this work. NMR studies were performed on a Varian Unity 500, which was partially funded by NIH Grant S10 RR06262, or an IBM AF200 spectrometer, which was purchased with funds from the NSF (PCM 8400801) and partially supported by funds from the University of Utah Cancer Center Core Grant (5P30 CA042014). Mass spectra were acquired on a Finnigan Mat 95, which was purchased with funds from NSF Grant CHE-9002690 and from the University of Utah Institutional Funds Committee.

Supplementary Material Available: ¹H and ¹³C spectra for makaluvamines A–F and for makaluvone (14 pages). Ordering information is given on any current masthead page.

(33) Kupchan, S. M.; Britton, R. W.; Ziegler, M. F.; Siegel, C. W. *J. Org. Chem.* 1973, 38, 178.

(34) Tano, K.; Shiota, S.; Remack, J. S.; Brent, T. P.; Bigner, D. D.; Mitra, S. *Mutat. Res.* 1991, 255, 175.

(35) Mossman, T. *J. Immunol. Methods* 1983, 65, 55.

(36) Swaffer, D. S.; Ireland, C. M.; Barrows, L. R. Submitted for publication.

(37) Muller, M. T.; Spitzner, J. R.; DiDonato, J. A.; Mehta, V. B.; Tsutsui, K.; Tsutsui, K. *Biochemistry* 1988, 27, 8369.

(38) Bradley, M. O.; Kohn, K. W. *Nucleic Acids Res.* 1979, 106, 793.